

## Charge-order breaking and ferromagnetism in $\text{La}_{0.4}\text{Ca}_{0.6}\text{MnO}_3$ nanoparticles

C. L. Lu, S. Dong, K. F. Wang, F. Gao, P. L. Li, L. Y. Lv, and J.-M. Liu<sup>a)</sup>

*Nanjing National Laboratory of Microstructures, Nanjing University, Nanjing 210093, China and International Center for Materials Physics, Chinese Academy of Sciences, Shenyang 110016, China*

(Received 3 May 2007; accepted 10 June 2007; published online 17 July 2007)

$\text{La}_{0.4}\text{Ca}_{0.6}\text{MnO}_3$  nanoparticles of grain size as small as  $\sim 20$  nm are prepared and their magnetic behaviors are investigated in order to understand the size effect of the charge ordering in manganites. The highly stable charge-ordered state can be significantly suppressed upon reduction of the grain size down to nanometer scale, while the ferromagnetism is enhanced. The magnetic phase separation due to the competition between ferromagnetic state and charge-ordered state as well as the surface spin disordering is responsible for the spin-glass-like state at low temperature.

© 2007 American Institute of Physics. [DOI: 10.1063/1.2753749]

Perovskite manganites with a general formula  $R_{1-x}A_x\text{MnO}_3$  (where  $R$  is rare earth and  $A$  is alkaline earth) have attracted attention not only for their potential applications but also for the intriguing fundamental problems associated with colossal magnetoresistance (CMR) effect and charge-ordered (CO) state.<sup>1-3</sup> The CO state, a real-space ordering of  $\text{Mn}^{3+}$  and  $\text{Mn}^{4+}$  ions and usually with antiferromagnetic (AFM) order, remains to be an essential ingredient of the physics of manganites.<sup>4</sup> It may be melted into ferromagnetic (FM) metallic state by external magnetic field, giving rise to the CMR effect,<sup>5</sup> although this CMR effect is somehow different from the conventional CMR originating from the double-exchange mechanism. However, the melting of the CO state usually requires high magnetic field, making practical applications of the CMR effect inaccessible. Thus, an alternative approach to destabilize the CO state is appealed.

Recently, quite a few experimental and theoretical studies focusing on the size effect of perovskite manganites were reported,<sup>6-14</sup> in which some interesting effects associated with the downsizing of the materials to tens of nanometers were revealed. One of these effects is the destabilization of the robust CO state as the ground state of bulk manganites. In consequence, a transition of the AFM order to the weak FM state was observed in both nanowires<sup>7</sup> and nanoparticles,<sup>8</sup> where the key role of the surface effect was argued. Similar prediction was made by considering the surface phase separation (PS) sequence,<sup>14</sup> although more relevant experimental evidence is required. Therefore, it would be of interest to investigate whether those manganites of the high CO stability have such significant size effect or not.

In this work, we studied the stability of the CO state and related magnetic behaviors of electron-doped  $\text{La}_{1-x}\text{Ca}_x\text{MnO}_3$  (LCMO) nanoparticles at  $x \sim 0.6$ , noting that earlier work was mainly on LCMO at  $x \sim 0.5$  where the CO state is associated with the charge exchange (CE) phase.<sup>13</sup> A choice of LCMO at  $x=0.6$  was based on the fact that LCMO is of intermediate bandwidth and shows tremendous CMR effect. For  $x > 0.5$ , LCMO is electron doped and the stability of the CO ground state increases with  $x$  and the maximal CO transition point is at  $x \sim 0.6$ . Thus, it is believed that the energy difference between the CO state and FM state is smaller than

that of the narrow bandwidth manganites.<sup>15,16</sup>

The LCMO nanoparticles at  $x=0.6$  were prepared by the facile sol-gel method.<sup>8</sup> At the end of the process, the gel was heated in a furnace at  $250^\circ\text{C}$  for about 10 h and porous materials were synthesized. In order to obtain samples of different average particle sizes, the powder was calcined at  $900^\circ\text{C}$  for 2 h and  $700^\circ\text{C}$  for 1 h, respectively, producing the final particles of  $\sim 60$  and  $\sim 20$  nm in average size, labeled as LCMO-60 and LCMO-20. For the comparison purpose, bulk LCMO (designated as LCMO-bulk) was prepared by the conventional solid-state reaction in air and the average grain size is about several microns and above. The samples were then characterized by x-ray diffraction (XRD), transmission electron microscopy (TEM). The magnetization  $M$  under conditions of zero-field cooling (ZFC) and field cooling (FC) was measured as a function of temperature  $T$  and magnetic field  $H$  using Quantum Design superconducting quantum interference device magnetometer. The magnetic loops for the LCMO-bulk were recorded at  $H=0-3$  T and  $T=3$  K and  $H=0-6.5$  T and  $T=50$  K, respectively, and the loops for LCMO-60 and LCMO-20 were measured at  $H=0-5$  T and  $T=3$  K.

The XRD patterns with clean background for all the samples, as shown in Fig. 1, can be indexed to a single orthorhombic crystal structure with the  $Pnma$  symmetry. Prechecking utilizing induction-coupled plasma analysis was made in order to exclude impurity in the samples. X-ray photoelectron spectroscopy was made and no  $\text{Mn}^{2+}$  ions were identified. Figures 2(a) and 2(b) present the typical TEM images for the LCMO-20 and the LCMO-60, confirming the particle sizes of  $\sim 20$  and  $\sim 60$  nm respectively. The HRTEM image obtained from a portion of an individual LCMO-60 nanoparticle [Fig. 2(c)] shows the clear lattice planes (the layer spacing is 0.271 nm, corresponding to the (200) planes or/and (121) planes) and thus indicates the well-crystallized structure inside the particle. The SAED image taken from individual particle of LCMO-60, as shown in Fig. 2(d), also reveals sharp diffraction spots.

Figure 3 presents the measured  $M$  as a function of  $T$  for the ZFC case and FC case with a magnetic field of 100 Oe. At a first glance, the detected  $M$  over the whole  $T$  range is very different from one and another for these samples no matter how the magnetic ordering is. When the LCMO-bulk sample shows its  $M \sim 10^{-2}$  emu/g, the value of  $M$  for the LCMO-60 and LCMO-20 is roughly two orders of magni-

<sup>a)</sup> Author to whom correspondence should be addressed; electronic mail: liujm@nju.edu.cn

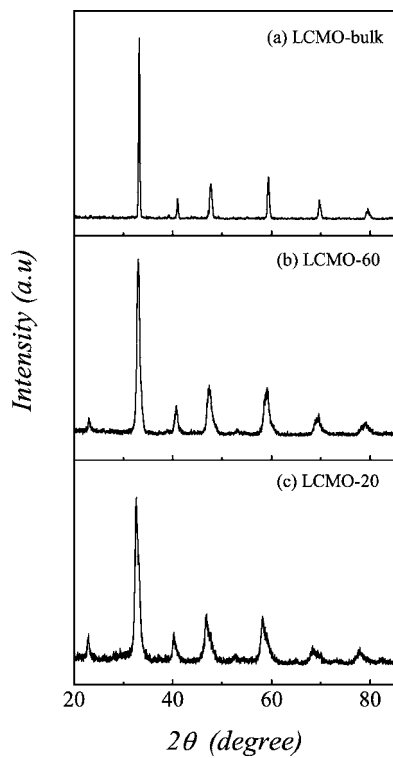


FIG. 1. XRD  $\theta$ - $2\theta$  spectra at room temperature for (a) the LCMO-bulk, (b) the LCMO-60, and (c) the LCMO-20, respectively.

tude larger. This tremendous difference refers to the fact that the dominant magnetic order in the LCMO-bulk sample is AFM type, while it is not the case for the LCMO-60 and LCMO-20. For details, the LCMO-bulk sample exhibits the typical CO peak at  $T_{CO} \sim 260$  K, consistent with earlier report.<sup>16</sup> The AFM transition is normally indicated by a much weaker feature with the Neel point  $T_N \sim 140$  K, although it is not clearly visible on the present scale. The nearly overlapped ZFC and FC  $M$ - $T$  curves over 50–300 K also confirm the AFM order. As  $T < 50$  K, the magnetization of the FC case is slightly larger than that of the ZFC case, indicating a canted AFM ground state.<sup>17</sup>

For the present nanoparticle samples, no clear CO transition is identified from the  $M$ - $T$  curves. Instead, a clear paramagnetic-FM transition can be identified and the Curie

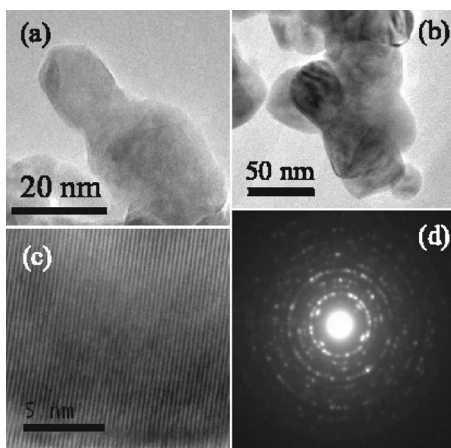


FIG. 2. Typical TEM images for (a) the LCMO-20 and (b) the LCMO-60, respectively. (c) The HRTEM pattern and (d) the SAED pattern of the LCMO-60 nanoparticles. The scale bar is 20 nm in (a), 50 nm in (b), and 5 nm in (c), respectively.

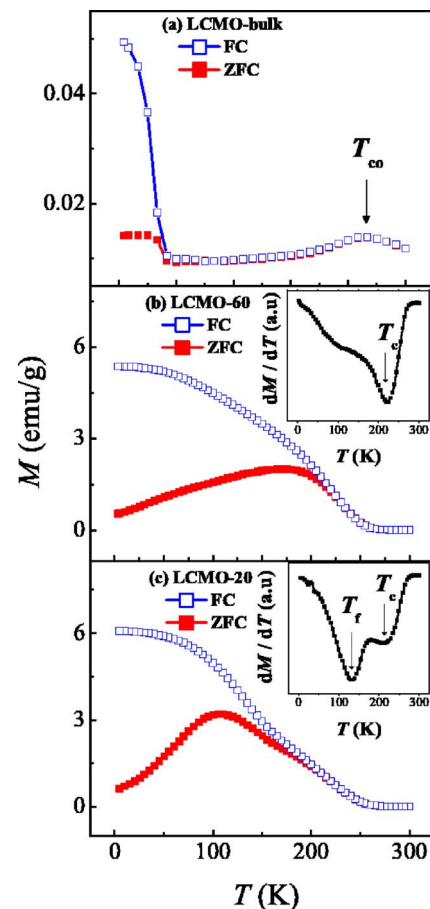


FIG. 3. (Color online) Measured  $M$  as a function of  $T$  under the conditions of ZFC and FC for (a) the LCMO-bulk, (b) the LCMO-60, and (c) the LCMO-20. The inset in (b) and (c) is the first derivative of  $M$  with respect to  $T$ .

point  $T_C$  for both the LCMO-60 and LCMO-20 is  $\sim 220$  K, determined by the inflection point defined by the minimum of  $dM/dT$ , as shown in the insets in Figs. 3(b) and 3(c), respectively. Furthermore, for both the LCMO-60 and LCMO-20, the tremendous difference between the ZFC curve and FC curve over a broad  $T$  range indicates the nature of spin-glass-like behaviors, although we have no intention to identify it as spin glass in the strict sense. In particular, a cusplike peak in the ZFC curve for the LCMO-20 sample can be observed, and the spin-glass-like transition temperature  $T = T_f \sim 120$  K, indicated by the arrow in the inset of Fig. 3(c).<sup>18</sup> A general argument is that the nanoparticles or nanowires have the surface spin-disordered magnetic state composed of noncollinear spin arrangement due to the reduced coordination and broken exchange bonds between surface spins.<sup>19</sup> Due to this magnetic frustration behavior, the spin-glass-like surface layer would contribute to the large difference between the ZFC and FC curves as well as the cusplike peak for the ZFC case.

We also measured the  $M$ - $H$  hysteresis for the LCMO-bulk at  $H=0$ –3 T and  $T=3$  K, and that at  $H=0$ –6.5 T and  $T=50$  K, respectively. The hysteresis for the LCMO-60 and LCMO-20 was obtained at  $H=0$ –5 T and  $T=3$  K, as plotted in Fig. 4. For the LCMO-bulk sample, the hysteresis is very thin and does not show any saturation as  $H$  is as large as 3 T. From the inset in Fig. 4(a), one notes that the CO state does not show any melting feature until  $H=6.5$  T at  $T=50$  K  $\ll T_{CO}$ . However, typical FM hysteresis can be observed for

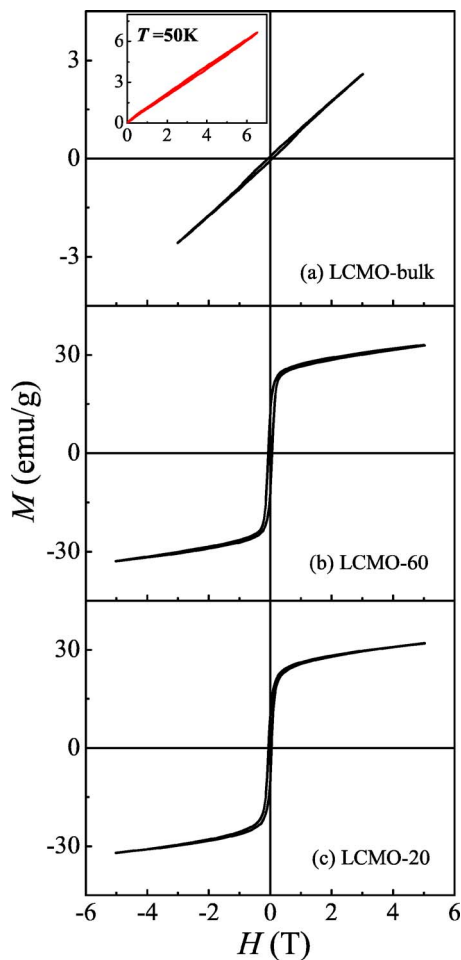


FIG. 4. (Color online) Measured  $M$  as a function of  $H$  for (a) the LCMO-bulk at 3 K (main panel) and at 50 K (the inset), (b) the LCMO-60 at 3 K, and (c) the LCMO-20 at 3 K.

the LCMO-60 and LCMO-20 samples, shown in Figs. 4(b) and 4(c), and the saturated  $M$ , as large as 25 emu/g, was recorded at  $H \sim 0.3$  T. It is known that if all spins at Mn sites aligned in the FM order, the maximum spin-only ordered moment would be  $3.4\mu_B$  per formula unit.<sup>18</sup> The measured  $M$  at  $T=3$  K and  $H=3$  T is  $\sim 1.0\mu_B$  per formula unit for both LCMO-60 and LCMO-20.

The standard models for manganites can be referred to understand the physics underlying the size effect.<sup>2</sup> It was predicted that the exchange parameters by which the FM/CO transition can occur depend on the dimension of the system.<sup>2</sup> Both the FM double exchange and the AFM superexchange are nearest neighboring (NN), while the NN number is determined by the dimension. As a result, the phase boundaries in the parameter space depend on the dimension, and the ground state of system might change from the CO state (as the case for the LCMO-bulk) toward a phase-separated state (as the cases for the LCMO-20 and LCMO-60) when the dimension is lowered. Based on this concept, a simplified surface PS model was proposed, which allows a rough esti-

mation of the FM amount in the nanoparticle system.<sup>14</sup> Given that this model was applied to the present LCMO system ( $x \sim 0.6$ ), if the critical magnetic field needed to melt the CO state is taken to be  $\sim 10$  T (our results show that the CO state remains stable against a field of 6.5 T at 50 K), the calculated FM fraction is  $\sim 25\%$  when the grain size is  $\sim 60$  nm and  $\sim 40\%$  when the size is  $\sim 20$  nm. The FM fraction estimated from the measured  $M$ - $H$  hysteresis at  $T=3$  K and  $H=3$  T is  $\sim 30\%$  for the LCMO-20 and LCMO-60, which has the same magnitude order as the value predicted by the surface PS model.<sup>14</sup> Nevertheless, it should be pointed out that this surface PS model is oversimplified and the calculated FM fraction may not be reliable in the quantitative sense, while the essential physics already lies in the standard models as mentioned above.

In addition, a clear  $T_f$  can be defined for the LCMO-20. The spin-glass-like behavior below  $T_f$  may originate from the phase separation. The decreasing of the size may affect significantly the magnetic properties of LCMO because of the broken exchange bonds between the surface Mn cations. However, while the size is small enough (e.g.,  $\sim 20$  nm), the effect of surface spin disordering would become more evident, and thus results in the spin-glass-like state at low  $T$ , although this spin-glass-like behavior is not very significant.

This work was supported by the Natural Science Foundation of China (50601013, 50528203), the National Key Projects for Basic Research of China (2006CB921802), and Nanjing University (2006CL1).

- <sup>1</sup>S. Jin, T. H. Tiefel, M. McCormack, R. A. Fastnacht, R. Ramesh, and L. H. Chen, *Science* **264**, 413 (1994).
- <sup>2</sup>E. Dagotto, T. Hotta, and A. Moreo, *Phys. Rep.* **344**, 1 (2001).
- <sup>3</sup>C. H. Chen and S.-W. Cheong, *Phys. Rev. Lett.* **76**, 4042 (1996).
- <sup>4</sup>J. B. Goodenough, *Phys. Rev.* **100**, 564 (1955).
- <sup>5</sup>Y. Tokura and Y. Tomioka, *J. Magn. Magn. Mater.* **200**, 1 (1999).
- <sup>6</sup>F. Chen, H. W. Liu, K. F. Wang, H. Yu, S. Dong, X. Y. Chen, X. P. Jiang, Z. F. Ren, and J.-M. Liu, *J. Phys.: Condens. Matter* **17**, L467 (2005).
- <sup>7</sup>S. S. Rao, K. N. Anuradha, S. Sarangi, and S. V. Bhat, *Appl. Phys. Lett.* **87**, 182503 (2005).
- <sup>8</sup>S. S. Rao, S. Tripathi, D. Pandey, and S. V. Bhat, *Phys. Rev. B* **74**, 144416 (2006).
- <sup>9</sup>Z. Q. Wang, F. Gao, K. F. Wang, H. Yu, Z. F. Ren, and J.-M. Liu, *Mater. Sci. Eng., B* **136**, 96 (2007).
- <sup>10</sup>A. Biswas and I. Das, *Phys. Rev. B* **74**, 172405 (2006).
- <sup>11</sup>A. Biswas, I. Das, and C. Majumdar, *J. Appl. Phys.* **98**, 124310 (2005).
- <sup>12</sup>K. S. Shankar, Sohini Kar, G. N. Subbanna, and A. K. Raychaudhuri, *Solid State Commun.* **129**, 479 (2004).
- <sup>13</sup>T. Zhang, C. G. Jin, T. Qian, X. L. Lu, J. M. Bai, and X. G. Li, *J. Mater. Chem.* **14**, 2787 (2004).
- <sup>14</sup>S. Dong, F. Gao, Z. Q. Wang, J.-M. Liu, and Z. F. Ren, *Appl. Phys. Lett.* **90**, 082508 (2007).
- <sup>15</sup>E. Dagotto, *Nanoscale Phase Separation and Colossal Magnetoresistance* (Springer, Berlin, 2003), 136, pp. 23–34.
- <sup>16</sup>A. Moreo, S. Yunoki, and E. Dagotto, *Science* **283**, 2034 (1999).
- <sup>17</sup>I. V. Solovyev and K. Terakura, *Phys. Rev. B* **63**, 174425 (2001).
- <sup>18</sup>K. F. Wang, Y. Wang, L. F. Wang, S. Dong, D. Li, Z. D. Zhang, H. Yu, Q. C. Li, and J.-M. Liu, *Phys. Rev. B* **73**, 134411 (2006).
- <sup>19</sup>R. H. Kodama, A. E. Berkowitz, E. J. McNiff, Jr., and S. Foner, *Phys. Rev. Lett.* **77**, 394 (1996).